Stress equivalence of solid-solution hardening

1990 J. Phys.: Condens. Matter 2 5797

(http://iopscience.iop.org/0953-8984/2/26/017)

J. Phys.: Condens. Matter **2** (1990) 5797–5808. Printed in the UK

Stress equivalence of solid-solution hardening

M Z Butt

Nuclear Research Laboratory, PO Box 1750, Government College, Lahore 54000, Pakistan, and International Centre for Theoretical Physics, PO Box 586, Trieste 34100, Italy

Received 23 October 1989, in final form 2 February 1990

Abstract. In the early 1970s, Basinski *et al* observed that, if two solid solutions of different solutes in a given solvent (copper or silver) had the same initial flow stress at a given temperature in the range 4–380 K, then they had the same activation volume. Moreover, two alloys based on the same solvent metal, which had the same initial flow stress and activation volume at a given temperature, would show the same temperature dependence of initial flow stress and activation volume throughout that range. These observations, which are known as the 'stress equivalence of solution hardening', have been shown to be readily accounted for in terms of the kink-pair formation model of solid-solution hardening.

1. Introduction

Some experiments of considerable potential implications in relation to solid-solution hardening (SSH) theory were carried out by Basinski *et al* [1] with alloy single crystals of high structural perfection and purity. The binary and ternary solid solutions used by them were of copper (with Al, Ag, Si and Ni) and silver (with In, Sn and Au), whereas the solute concentration ranged from 0.01 to 20 at.%. They found that, if some solid solutions of different solutes in any of these two solvent metals had the same critical resolved shear stress (CRSS) at a given temperature in the range 4–380 K, then they had the same activation volume as well. Moreover, alloys with the same CRSS at a given temperature had coincident values of the CRSS at all other temperatures in the range studied; a similar correlation holds for the temperature dependence of the activation volume. Basinski *et al* [1] termed these features 'stress equivalence of solution hardening'. They also inferred from their experimental data that a single mechanism, independent of the particular interaction between dislocations and solute atoms, was responsible for SSH in close-packed metals and that SSH theories would have to be based on models in which the unit activation process involves the interaction between a dislocation and many solute atoms, except probably in rather dilute alloys.

The observations referred to above, among others, are of basic significance, for any adequate theory of SSH must be able to account for them. As the parameters studied by Basinski *et al* [1] could be defined analytically within the framework of the kink-pair formation (KPF) model of SSH [2–4], it seemed desirable to examine how far the phenomenon of 'stress equivalence of solution hardening' could be explained by the model, the basic features of which we shall first briefly highlight.

0953-8984/90/265797 + 12 $03.50

2. The KPF model

In the KPF model of SSH, initially proposed by Feltham [2] for concentrated solid solutions based on metals with a low Peierls potential and later found to be applicable also to dilute solid solutions [5–8], the elementary activation process, reviewed in detail by Feltham and Kauser [7], comprises stress-assisted, thermally activated unpinning of edge-dislocation segments from short rows of solute-atom pinning points at the CRSS τ, which varies with temperature T and solute concentration c, as given by the relation [4]

$$\tau = \tau_0 \exp(-W/W_0) \qquad \tau_0 = 4Uc^{*1/2}/nb^3 \qquad W_0 = n(Gb^3Uc^{*1/2})^{1/2} \tag{1}$$

with

$$W = mkT \qquad m = \ln(\dot{\gamma}_0/\dot{\gamma}). \tag{2}$$

Here τ_0 is the CRSS as $T \rightarrow 0$ K, G is the shear modulus, b is the length of the Burgers vector, k is the Boltzmann constant and U is, in the tight-binding approximation used, the energy expended per solute atom for the initial breakaway of a dislocation segment from a group of such aligned pinners in the process of nucleation of a kink pair; m is a constant proportional to the logarithm of the deformation rate $\dot{\gamma}$ and is usually equal to about 25; W represents the stress-reduced barrier height or activation energy (free enthalpy) of formation of a kink pair, akin to the 'bulge' referred to by Arsenault and Cadman [9], and W_0 has been shown [10, 11] to be numerically equal to

(i) the energy of interaction between the dislocation segment of length $L_0 = b(4Gn/\tau_0)^{1/2}$ involved in the unit activation process and solute atoms close to it,

(ii) the increase in line energy of the unpinned dislocation segment of initial length L_0 during the formation of a kink pair of maximum height nb, and

(iii) one half of the work done by the applied shear stress τ_0 in moving the dislocation segment after its breakaway from solute-atom pinning points, over the mean displacement $\frac{1}{2}nb$ in an activated jump.

An effective concentration $c^* = c + c_0$ has been used in equation (1) instead of the solute concentration c because the contribution to c^* made by the 'equivalent' concentration c_0 [12] allows semi-empirically for the presence in the crystals of barriers to dislocation motion other than the solute atoms and leads to a non-zero CRSS for $c = 0$, providing a measure of the resistance of the unalloyed crystal to plastic flow. Numerically, c_0 is equal to the common intercept on the negative c axis made by the extrapolated τ versus c isotherms. The term $Uc^{*1/2}$ therefore represents the binding energy per unit length of dislocation with the 'effective' pinning points in the alloy. Except for rather dilute alloys, c_0 may usually be omitted.

For the temperature and concentration dependences of the activation volume v, customarily defined as $(-\partial W/\partial\tau)_T$ or $kT[\partial \ln\dot{\gamma}/\partial\tau]_T$, one can readily find from equations (1) and (2) that

$$v = v_0 \exp(W/W_0) \qquad v_0 = \tfrac{1}{4}b^3n^2(Gb^3/Uc^{*1/2})^{1/2}. \tag{3}$$

It should be noted that equations (1) and (3) are convenient representations of the somewhat complex expressions given in [3] and prove adequate up to temperatures where, owing to the occurrence of diffusional recovery processes in the crystal, the model used would cease to be applicable. From equations (1) and (3) we also find that for a given alloy the product τv is constant, i.e.

$$\tau v = \tau_0 v_0 = W_0. \tag{4}$$

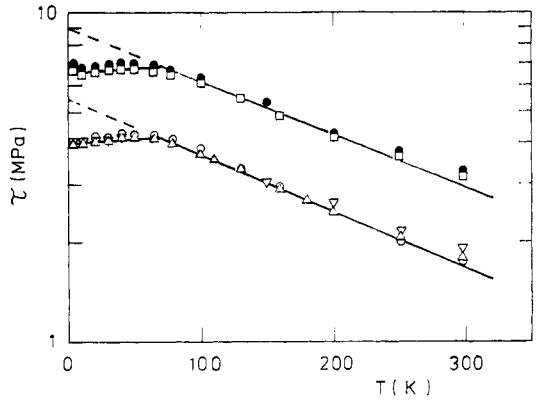

Figure 1. The CRSS of some copper-based alloys as a function of temperature in a log–linear representation where the symbols denote the data obtained by Basinski *et al* [1]: ●, Cu–0.5 at.% Al–0.1 at.% Ag; □, Cu–1.0 at.% Al; △, Cu–0.5 at.% Al; ○, Cu–0.1 at.% Ag; ▽, Cu–0.5 at.% Si.

3. Comparison with experimental data

Reference to figure 1 shows the temperature dependence of the CRSS for some copper-based alloys corresponding to two levels of solution hardening. Disregarding the deviation from the generally expected behaviour below a certain temperature $T_0 \simeq 70$ K, the straight lines drawn through the τ versus T data points taken from [1] and plotted on log–linear coordinates yield W_0 on using equation (1) in the form $\mathrm{d}(\ln \tau)/\mathrm{d}T = -mK/W_0$, and τ_0 as the intercepts made by them on the stress axis by extrapolation. The values of W_0 and τ_0 thus obtained, along with those for other copper-based alloys deformed by Basinski *et al* [1], are given in table 1.

Concerning the anomalous mechanical response observed at $T < 70$ K (figure 1), which is usually associated with Granato's inertial effects criticised by Feltham [13] for various reasons, it will be shown to be explicable in terms of the deformation-induced enhancement of local stresses at barriers to the movement of dislocations [14–29] at temperatures sufficiently low to reduce thermal recovery to comparatively low levels. In FCC metals the effect seems to arise mainly as a consequence of mutual attraction between two arms of the 'hairpin' in glide dislocations pinned under stress in Orowan configurations at strong obstacles [14, 27]. The stress τ in the relations describing deformation kinetics, e.g. in equation (1), has then to be multiplied by a stress-concentration factor $f(T)$, which for 'hairpin' configurations is estimated to lie between 1 and 4 [14, 27], its value increasing with decreasing temperature.

In the case of solid solutions, the anomalies are similar to those observed in pure metals, and the Bacon–Scattergood [14] 'hairpin' mechanism is expected to be operative at low temperatures. However, the arms of the dislocations forming the cusp are now impeded in their motion by pinning with dispersed solute atoms; the attractive interaction between the arms is consequently reduced, as pinners (i.e. solute atoms) oppose mutual attraction. This leads to a reduction in the value of $f(T)$ compared with that estimated for pure metals. The evidence obtained by Feltham and Kauser [7], Ghauri *et al* [23] and Butt *et al* [29] in the case of Cu–Zn (c = 0.03–1.0 at.% Zn), Cu–Zn (c = 12–35 at.% Zn) and Cu–Mn (c = 0.11–7.6 at.% Mn) alloys, respectively, lends support to this proposal.

Now the τ versus T data for the alloys referred to in figure 1 have been depicted in linear–linear coordinates in figure 2. The curves drawn through the data points comply with equation (1) in which the values of c^*, τ_0 and W_0 taken from table 1 were used and, below the peak temperature $T_0 \simeq 70$ K, τ was multiplied by a stress-concentration factor

Table 1. Values of various parameters of the KPF model of SSH derived from the experimental data obtained by Basinski *et al* [1] with copper-based alloys. $G = 4.5 \times 10^4$ MPa, $b = 2.54 \times 10^{-10}$ m and $Gb^3 = 4.6$ eV in all cases.

Alloy	Designation	c (at.%)	c^* (at.%)	τ_0 (MPa)	W_0 (meV)	n	U (meV)	$Uc^{*1/2}$ (meV)	L_0 (units of b)	v_0 (units of b^3)	N
Cu–Al	A	0.01	0.04	0.68	299	10.3	9.2	0.2	1651	4194	17
	B	0.05	0.08	1.36	398	9.9	12.4	0.4	1145	2806	26
	C	0.10	0.13	2.00	404	8.7	13.0	0.5	885	1875	28
	D	0.25	0.28	3.6	461	7.9	14.0	0.7	628	1229	31
	E	0.50	0.53	5.5	500	7.2	14.4	1.0	485	870	34
	F	1.00	1.03	9.0	528	6.4	14.6	1.5	358	561	36
	G	1.40	1.43	11.6	597	6.4	15.8	1.9	315	505	37
	H	1.85	1.88	14.5	608	6.0	16.3	2.2	273	410	37
	I	2.80	2.83	19.2	629	5.6	16.3	2.7	229	321	38
	J	4.60	4.63	23.6	661	5.4	15.1	3.2	203	274	43
	K	5.60	5.63	25.6	673	5.3	14.8	3.5	193	254	46
	L	7.40	7.43	27.2	671	5.2	13.3	3.6	186	241	50
	M	9.20	9.23	31.0	639	4.8	12.7	3.9	167	199	51
	N	11.00	11.03	37.0	612	4.4	12.7	4.2	146	160	49
Cu–Ag	O	0.05	0.08	4.0	479	7.9	28.9	0.8	596	1183	13
	P	0.10	0.13	5.5	500	7.2	29.1	1.0	485	870	15
	Q	0.19	0.22	9.6	549	6.4	33.9	1.6	346	549	15
Cu–Ni	R	5.00	5.03	11.4	598	6.4	8.4	1.9	318	504	71
Cu–Si	S	0.50	0.53	5.5	500	7.2	14.4	1.0	485	870	34
Cu–0.5 at.% Al–0.1 at.% Ag											
	T	0.60	0.63	9.0	528	6.4	18.7	1.5	358	561	28
Cu–5.6 at.% Al–0.34 at.% Ag											
	U	5.94	5.97	37.0	612	4.4	17.3	4.2	146	160	36

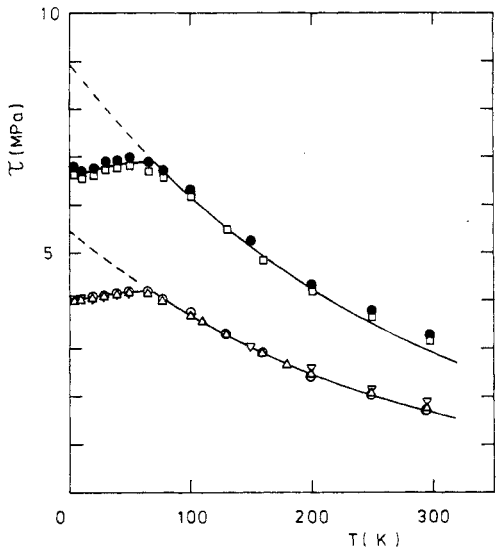

Figure 2. The temperature dependence of the copper-based alloys referred to in figure 1. The theoretical curves drawn through the data points were obtained by means of equation (1) in which τ was replaced by $\tau(T' + T_0)/(T' + T)$ below a certain temperature $T_0 = 70$ K at which deviations from the generally expected τ versus T behaviour sets in; the values of T' used were 190 and 185 K for the top and bottom curves, respectively, whereas those of τ_0 and W_0 are given in table 1.

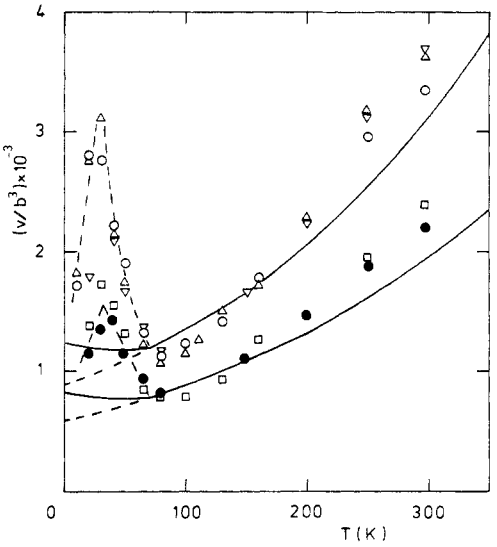

Figure 3. The temperature dependence of the activation volume for the copper-based alloys referred to in figures 1 and 2. The full curves comply with equation (3) in which v was replaced by $v(T' + T)/(T' + T_0)$ below $T_0 = 70$ K, and the values of T', W_0 and v_0 used were the same given in the caption to figure 2.

$f(T) = (T' + T_0)/(T' + T)$, T' being a constant sensitive to the amount and mode of solute distribution in the crystal (see, e.g., [23, 28, 29]), to make allowance for the self-stress of dislocations at rather low temperatures. The value of $f(T)$ used here ranges from 1 to 1.4, the latter being smaller, in accord with the expectation, than that estimated for pure FCC metals [14].

Similarly the points in figure 3 denote the experimental values of the activation volume $v = kT[\partial(\ln \dot{\gamma})/\partial\tau]_T$ appertaining to two levels of solution hardening referred to in figures 1 and 2, as a function of temperature, whereas the full curves are theoretical, i.e. obtained by means of equation (3) using the values of W_0 and v_0 (table 1), and dividing v by $f(T) = (T' + T_0)/(T' + T)$ below a certain temperature $T_0 \simeq 70$ K (since $v \propto 1/\tau$ as per equation (4)) to encompass the anomalous behaviour at low temperatures.

Figure 4 shows the dependence of the activation volume on the CRSS at 78 and 298 K; the curves represent, within experimental error, the data of Basinski *et al* [1] for 22 copper-based alloys; the points are theoretical, i.e. obtained as described above with the parameters given in table 1. It should be noted that, as the points denoting the calculated values for the alloys labelled S, T and U (table 1) are coincident with those for alloys E, F and N, respectively, they have been omitted for clarity. One observes that the KPF model accounts rather well for the temperature dependence of the CRSS and of the associated activation volume, except for somewhat uncertain detail appertaining to low temperatures in figure 3, where the concept of deformation-induced enhancement of local stress may account, in part at least, for the discrepancies.

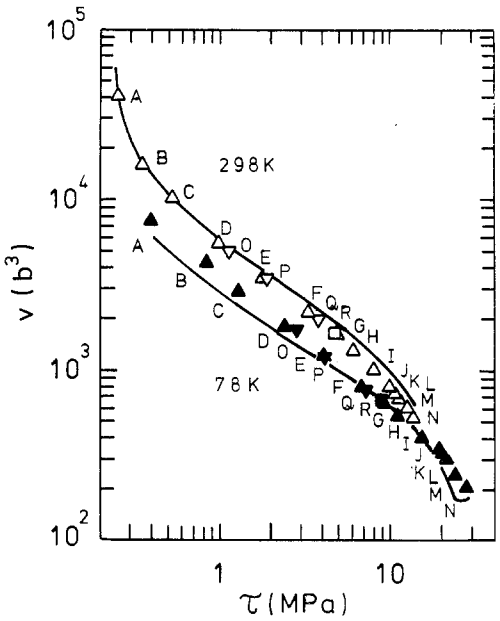

Figure 4. The dependence of the activation volume on the CRSS and on the temperature for Cu–Al (△), Cu–Ni (□) and Cu–Ag (▽) alloys. The curves represent the experimental data of Basinski *et al* [1] whereas the symbols denote theoretical values computed with the help of equations (1) and (3) using the parameters given in table 1.

Knowing the values of W_0, τ_0 and c^*, one can obtain n and U using the relations

$$n^3 = (W_0^2/\tau_0)[4G/(Gb^3)^2] \tag{5}$$

$$U = W_0^2/Gb^3n^2c^{*1/2} \tag{6}$$

which are readily derivable from the basic definitions of W_0 and τ_0 in terms of n and U (equation (1)). The values of n and U thus obtained facilitate the determination of $Uc^{*1/2}$ (the binding energy per unit length of dislocation with the effective pinning points in the alloy), L_0 (the initial length of the dislocation segment involved in the unit activation process as $T \rightarrow 0$ K) and $N = L_0/\lambda$ (the number of alloy atoms with which the dislocation segment L_0 is initially pinned prior to the nucleation of a kink pair of maximum height nb) where $\lambda = b/c^{1/2}$ is the average spacing between neighbouring alloy atoms; the values for copper- and silver-based alloys deformed by Basinski *et al* [1] are given in tables 1 and 2, respectively. It should be noted that $N \gg 1$ for each alloy containing solute atoms in the range 0.01–20 at.%, which means that Friedel's breakaway from individual pinners is unlikely even for the most dilute alloy referred to.

Concerning the 'stress equivalence of solution hardening', i.e. the superimposition of the τ versus T curves of solid solutions with the same base but different solutes, equation (1) yields the conditions

$$(\tau_0)_1 = (\tau_0)_2 = (\tau_0)_3 = \ldots \tag{7}$$

and

$$(W_0)_1 = (W_0)_2 = (W_0)_3 = \ldots \tag{8}$$

or, in terms of n and U [7],

$$n_1 = n_2 = n_3 = \ldots \tag{9}$$

and

$$(Uc^{*1/2})_1 = (Uc^{*1/2})_2 = (Uc^{*1/2})_3 = \ldots. \tag{10}$$

Table 2. Values of various parameters of the KPF model of SSH derived from the experimental data obtained by Basinski *et al* [1] with silver-based alloys. $G = 2.7 \times 10^4$ MPa, $b = 2.89 \times 10^{-10}$ m and $Gb^3 = 4.0$ eV in all cases.

Alloy	Designation	c (at.%)	c^* (at.%)	τ_0 (MPa)	W_0 (meV)	n	U (meV)	$Uc^{*1/2}$ (meV)	L_0 (units of b)	v_0 (units of b^3)	N
Ag–In	a	0.01	0.03	0.50	738	19.4	20.9	0.4	2047	9918	21
	b	0.05	0.07	0.68	874	19.6	18.8	0.5	1764	8590	39
	c	0.10	0.12	1.3	617	12.5	17.6	0.6	1019	3163	32
	d	0.20	0.22	1.75	630	11.5	16.0	0.8	842	2415	38
	e	0.50	0.52	3.60	664	9.4	17.3	1.3	531	1250	38
	f	1.0	1.02	5.6	687	8.3	17.0	1.7	400	831	40
	g	2.5	2.52	11.0	767	7.1	18.4	2.9	264	466	42
	h	0.28	0.30	2.50	743	11.4	19.4	1.1	702	1996	37
	i	0.45	0.47	3.70	714	9.8	19.4	1.3	535	1317	36
	j	0.95	0.97	6.60	677	7.8	19.1	1.9	357	702	35
Ag–Sn	k	0.03	0.05	1.9	607	10.9	34.7	0.8	787	2127	14
	l	0.08	0.10	3.3	639	9.4	36.5	1.2	555	1303	16
	m	0.25	0.27	7.0	670	7.6	37.4	1.9	342	656	17
	n	0.50	0.52	11.9	536	5.5	32.9	2.4	223	311	16
	o	0.60	0.62	13.4	518	5.1	32.8	2.6	203	256	16
Ag–Au	p	10.0	10.02	4.70	763	9.4	5.2	1.7	465	1088	147
	q	20.0	20.02	6.40	843	9.1	4.8	2.2	392	892	175

The numerical data given in tables 1 and 2 lend substance to these relations. Moreover, equations (7) and (8) in conjunction with equation (4) suggest that solid solutions of different solutes in a given solvent metal, which exhibit identical τ versus T behaviour, will also satisfy the condition

$$(v_0)_1 = (v_0)_2 = (v_0)_3 = \ldots \tag{11}$$

and hence these will have a common v versus T curve (equation (3)) as well. This inference is borne out by the v versus T measurements (figure 3) made by Basinski *et al* [1] with the copper-based alloys. It should be, however, remembered that, in the case of stress-equivalent solid solutions in which the CRSS versus T anomaly occurs, the condition [7]

$$f_1(T) = f_2(T) = f_3(T) = \ldots \tag{12}$$

has to be added to equations (7) and (8) for $T \leqslant T_0$. Deviations from stress equivalence compatible with failure of this criterion have been observed with copper single crystals containing either manganese or germanium in solid solution [30].

It is worthy of note that the concept of the stress equivalence of solution hardening is also partly explicable [31–33] on the basis of the revised versions of the models of Labusch [34] and Nabarro [35], although there are clear discrepancies between the observed and the predicted temperature dependences of the flow stress. In the models referred to, the length of the dislocation segment involved in a unit activation process and the CRSS at 0 K are governed by the parameters cf_m^2 and w, where f_m is the maximum force of interaction between a solute atom and a dislocation and w is the range of this force. The parameters cf_m^2 and w appear as a ratio in the expression for the dislocation length and as a product in that for the CRSS at 0 K. Thus two solid solutions of different solutes in a given solvent metal will have identical values of τ_0 if $(cf_m^2)_1 = (cf_m^2)_2$ and $w_1 = w_2$; this is analogous to the stress-equivalence rules enunciated by equations (9) and (10). However, if the low-temperature effects, whether inertial or non-inertial, also contribute to the CRSS, then two solid solutions with identical values of cf_m^2 and w will not be stress equivalent unless the low-temperature contributions are also identical (e.g. equation (12)). This criterion is not encompassed by the Labusch [34] and Nabarro [35] models. Similarly the stress dependence of the activation volume in copper- and silver-based alloys predicted at 0 K by Nabarro [31] does not correlate with that observed at 78 and 298 K by Basinski *et al* [1]; the predicted value of exponent p in the relation $v \propto \tau^{-p}$ is $\frac{1}{2}$ in the Labusch regime and 2 in the Friedel limit, whereas the observed values are about $\frac{2}{3}$ and 1 for copper alloys and $\frac{2}{3}$ for silver alloys in the Labusch regime while the situation is not clear in the so-called Friedel limit. Also, the abrupt vertical step predicted in the theoretical v_0 versus τ_0 curve at rather high stresses due to a change from a regime in which the two partials of a dissociated dislocation move in a coordinated manner to a regime in which the partials move independently is not observed experimentally.

Reverting to the KPF model, figures 5(*a*) and 5(*b*) show the correlations between $\tau(T_1) - \tau(T_2)$ and $\tau(T_1)$, with $T_1 = 78$ K and $T_2 = 298$ K, for copper- and silver-based alloys, respectively. Here the points denoted by letters were obtained by means of the relation [18]

$$[\tau(T_1) - \tau(T_2)]/\tau(T_1) = 1 - \exp[-(mk/W_0)(T_2 - T_1)] \tag{13}$$

and the curves represent, within experimental error, measured values [1]. These were rather close to the corresponding values determined on the basis of the data given in the tables and have been omitted for clarity. Again, as the theoretical points for alloys S, T and U (table 1) are coincident with those for alloys E, F and N, respectively, they have not been shown in figure 5(*a*). A similar correlation can also be shown to hold for

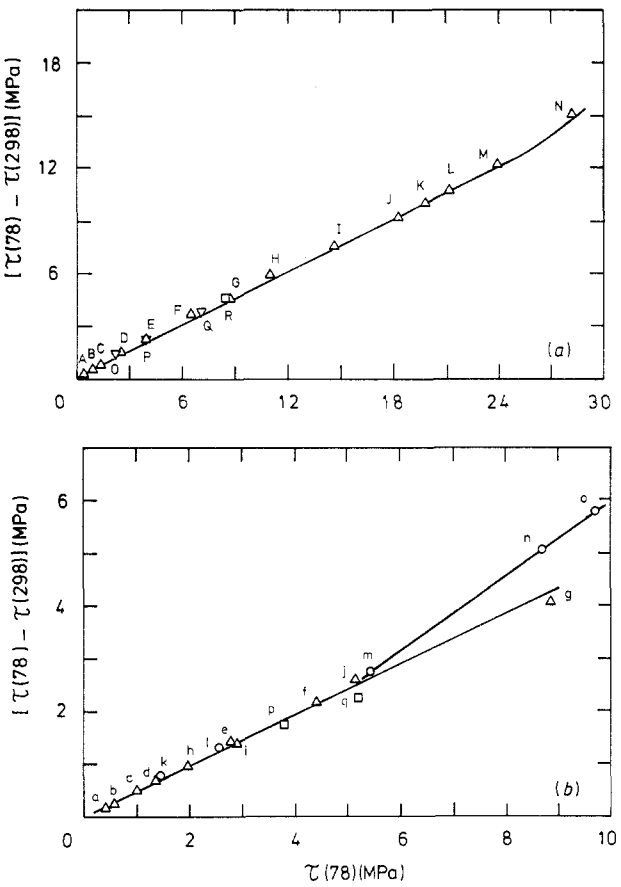

Figure 5. The dependence of $\tau(78)-\tau(298)$ on $\tau(78)$ for the (*a*) copper-based alloys (△, Cu–Al; □, Cu–Ni, ▽, Cu–Ag) and (*b*) silver-based alloys (△, Ag–In; ○, Ag–Sn; □, Ag–Au) referred to in tables 1 and 2, respectively. The full curves were drawn through experimental values [1] (not shown); the points were determined by means of equation (13) with the data given in the tables.

$v(T_2) - v(T_1)$ and $v(T_1)$ in accord with the expression

$$[v(T_2) - v(T_1)]/v(T_1) = \exp[(mk/W_0)(T_2 - T_1)] - 1 \tag{14}$$

which has been derived from equation (3).

Reference to figure 5(*b*) shows loss of stress equivalence in the case of Ag–Sn ($c > 0.25$ at.% Sn) alloys. Butt and Shami [36] have examined this problem in considerable detail for numerous copper- and silver-based alloys and found that it seems to be related to the change in the observed value of the exponent r in the relation $\tau \propto c^r$ with temperature. In fact deviations from random distribution of solute atoms occur in solid-solution crystals, which contain either a high concentration of solute atoms of small size-misfit factor $\delta = (1/b)(\mathrm{d}b/\mathrm{d}c)$ or even a low concentration of solute atoms with large δ-values [8, 37]; the change in the mode of solute distribution *inter alia* influences the temperature and concentration dependences of the CRSS of solid solutions [6, 11, 31, 38] and hence contributes to the loss of stress equivalence.

Now, for a given change in the test temperature $\Delta T = T_2 - T_1$ of an alloy, one can readily find from equations (13) and (14) an expression for the product of accompanying

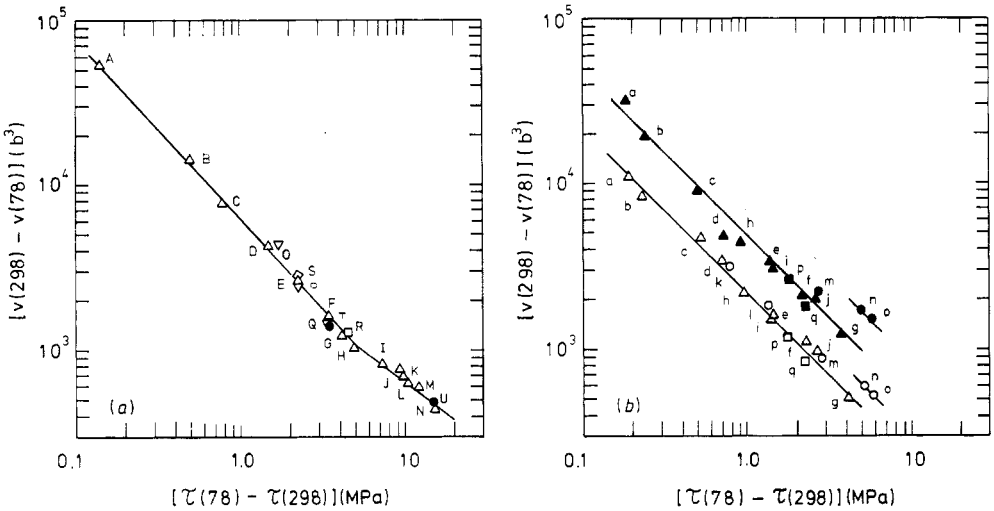

Figure 6. The relation between $v(298)$–$v(78)$ and $\tau(78)$–$\tau(298)$ for the (*a*) copper-based alloys (△, Cu–Al; □, Cu–Ni; ▽, Cu–Ag; ◇, Cu–Si; ●, Cu–Al–Ag) and (*b*) silver-based alloys (△, Ag–In; ○, Ag–Sn; □, Ag–Au) referred to in tables 1 and 2, respectively. In (*a*) the symbols denote the experimental values of Basinski *et al* [1]; as the theoretical values obtained by the use of equation (15) are close to the experimental values, they have been omitted. In (*b*) the full symbols represent experimental data taken from [1]; the open symbols are theoretical, i.e. computed through equation (15) by use of data given in table 2.

changes $\Delta\tau = \tau(T_1) - \tau(T_2)$ in the CRSS and changes $\Delta v = v(T_2) - v(T_1)$ in the associated activation volume. It is given by

$$\Delta\tau\,\Delta v = 2W_0[\cosh(mk\,\Delta T/W_0) - 1]. \tag{15}$$

Thus figures 6(*a*) and 6(*b*) refer to the dependence of $\Delta v = v(T_2) - v(T_1)$ on $\Delta\tau = \tau(T_1) - \tau(T_2)$, with $T_1 = 78$ K and $T_2 = 298$ K for copper- and silver-based solid solutions, respectively. The experimental values of Basinski *et al* [1] for copper-based alloys have been denoted by symbols in figure 6(*a*); those derived by means of equation (15) on using the data given in table 1 were found to be close to the experimental values and have been omitted for clarity. Similarly, the full symbols in figure 6(*b*) denote the data of Basinski *et al* [1] for silver-based alloys whereas the open symbols were determined by means of equation (15) in which the data given in table 2 were used. Although the experimental values of Δv in figure 6(*b*) are somewhat higher than the calculated values, most probably owing to the occurrence of possible diffusional effects at room temperature, yet the functional form of Δv versus $\Delta\tau$ can be seen to be the same in theory and experiment.

On the other hand, although Nabarro derived in his recent paper [32] a power law for the stress dependence of the activation volume ($v_0 \propto \tau_0^{-2/3}$) in the Labusch regime better than the earlier law ($v_0 \propto \tau_0^{-1/2}$) [31], yet the theoretical value of $\Delta v = v(298) - v(78)$ at a given stress level due to the temperature change $\Delta T = 220$ K was found to be extremely small compared with the experimental value in the case of silver-based alloys, and even negative for copper-based alloys. This clearly indicates, as remarked by Nabarro [32], the inability of the Labusch and Nabarro models to predict the temperature dependence of the CRSS and of the activation volume correctly.

Finally, it is evident from figures 5 and 6 that for alloys based on a given metal

(i) the change $\tau(T_1) - \tau(T_2)$ in the CRSS, due to increase in temperature from T_1 to T_2 is equivalent to the CRSS $\tau(T_1)$ and

(ii) the change $v(T_2) - v(T_1)$ in the associated activation volume is equivalent to the change $\tau(T_1) - \tau(T_2)$ in the CRSS.

However, Ag–0.5 at.% Sn and Ag–0.6 at.% Sn alloys, denoted by letters n and o respectively, which do not satisfy the stress-equivalent conditions (equations (7), (8) and (11)), as one can readily verify from the numerical data given in table 2, are exceptions to it.

4. Conclusions

One may conclude from the foregoing considerations that the 'stress equivalence of solution hardening', i.e. correlation of the data for both the temperature and the strain-rate dependence of the CRSS of alloys with the amount of solution hardening rather than with the concentration and type of solute, is fully explicable in terms of the KPF model of SSH. Also, in accord with the conviction of Basinski *et al* [1], a single mechanism of SSH, which involves the interaction between a dislocation and several solute atoms, is operative in dilute as well as in concentrated alloys, except possibly in alloys with solute content below about 100 ppm.

Acknowledgments

The author is grateful to Professor Abdus Salam NL and the Swedish Agency for Research Cooperation with Developing Countries for hospitality at the International Centre for Theoretical Physics, Trieste, Italy, where most of this work was done during his visit in the capacity of Associate Member. He is also indebted to the referees for their constructive criticism of the earlier version of this paper.

References

[1] Basinski Z S, Foxall R A and Pascual R 1972 *Scr. Metall.* **6** 807
[2] Feltham P 1968 *J. Phys. D: Appl. Phys.* **1** 303
[3] Butt M Z and Feltham P 1978 *Acta Metall.* **26** 167
[4] Butt M Z, Feltham P and Ghauri I M 1986 *J. Mater. Sci.* **21** 2664
[5] Butt M Z 1989 *Phil. Mag. Lett.* **60** 141
[6] Butt M Z and Khan M A 1989 *Phys. Status Solidi* a **113** K189
[7] Feltham P and Kauser N 1990 *Phys. Status Solidi* a **117** 135
[8] Butt M Z 1989 *Solid State Commun.* **72** 139
[9] Arsenault R J and Cadman T W 1978 *Rev. Deform. Behav. Mater.* **3** 5
[10] Butt M Z 1988 *J. Mater. Sci. Lett.* **7** 879
[11] Butt M Z and Ghauri I M 1988 *Phys. Status Solidi* a **107** 187
[12] Feltham P 1973 *Mater. Sci. Eng.* **11** 118
[13] Feltham P 1980 *Phys. Status Solidi* b **98** 301
[14] Bacon D J and Scattergood R O 1977 *Rev. Deform. Behav. Mater.* **2** 317
[15] Feltham P 1979 *Scr. Metall.* **13** 119
[16] Raza S M 1982 *Scr. Metall.* **16** 1325
[17] Feltham P 1983 *Phys. Status Solidi* a **75** K95
[18] Butt M Z, Feltham P and Raza S M 1983 *Scr. Metall.* **17** 1337
[19] Feltham P and Butt M Z 1984 *Cryst. Res. Technol.* **19** 325
[20] Butt M Z, Feltham P and Raza S M 1984 *Phys. Status Solidi* a **84** K125

[21] Butt M Z and Feltham P 1985 *J. Mater. Sci. Lett.* **4** 302
[22] Ahmad M, Butt M Z, Chaudhary S A and Ghauri I M 1986 *Phil. Mag.* A **54** L9
[23] Ghauri I M, Feltham P and Butt M Z 1986 *Phys. Status Solidi* a **96** K43
[24] Butt M Z, Feltham P and Raza S M 1987 *Phil. Mag. Lett.* **55** 59
[25] Butt M Z and Raza S M 1987 *J. Mater. Sci. Lett.* **6** 54
[26] Jonsson S and Beuers J 1987 *Mater. Sci. Eng.* **91** 111
[27] Feltham P 1988 *Phil. Mag.* B **57** 111
[28] Butt M Z, Chaudhary S A and Ghauri I M 1989 *Mater. Lett.* **7** 347
[29] Butt M Z, Rafi Z and Khan M A 1990 *Phys. Status Solidi* a at press
[30] Wille T, Gieseke W and Schwink C 1987 *Acta Metall.* **35** 2697
[31] Nabarro F R N 1982 *Proc. R. Soc.* A **381** 285
[32] Nabarro F R N 1985 *Phil. Mag.* B **52** 785
[33] Nabarro F R N 1985 *Dislocations and Properties of Real Materials* (London: Royal Society) p 152
[34] Labusch R 1972 *Acta Metall.* **20** 917
[35] Nabarro F R N 1977 *Phil. Mag.* **35** 613
[36] Butt M Z and Shami M A 1988 *J. Mater. Sci.* **23** 2661
[37] Schwink Ch and Wille Th 1980 *Scr. Metall.* **14** 1093
[38] Arsenault R J and Esterling D M 1985 *Dislocations in Solids* ed H Suzuki, T Ninomiya, K Sumino and S Takeuchi (Tokyo: University of Tokyo Press) p 199